Order-Disorder Transitions in the Vanadium-Hydrogen System Measured by Perfect-Crystal Neutron Small-Angle Scattering*

A. Mikšovsky, H. Rauch, E. Seidl, and W. Wachter
Atominstitut der Österreichischen Universitäten, Wien, Austria

Z. Naturforsch. **39 a,** 1077 – 1081 (1984); received July 31, 1984

The solubility limits for hydrogen in vanadium were determined using small-angle neutron scattering. In addition, the neutron transmission in dependence of the hydrogen concentration at 170 °C (pure α-phase) and at 20 °C ($\alpha + \beta$-phase) was measured. The total cross section of the proton in the α-phase was found to be nearer to the free than to the bound value. The Guinier-approximation is used to examine the small-angle scattering of precipitates in the β-phase V_2H. The features of perfect-crystal neutron small-angle scattering for the precise transmission measurement and for the investigation of the very small Q-range are demonstrated.

1. Introduction

In recent years numerous measuring techniques have been employed to determine the phase boundaries of metal-hydrogen systems [1]. X-ray, neutron and electron diffraction methods [2–5] have been used to study structural changes which occur when phase transitions take place. Other methods exploit the change of macroscopic physical properties, such as electrical resistivity [6], superconductivity [7], internal friction [8], NMR [9], differential thermal analysis [10] etc. The applicability of the neutron scattering technique is based on the rather high scattering cross section of hydrogen and deuterium and its sensitivity to structural changes.

A neutron beam traversing a metal-hydrogen sample will be attenuated by absorption and scattering processes and will be broadened due to neutron small-angle scattering (SANS) if precipitates exist. Experimentally the onset of precipitation can easily be detected by cooling a sample from the α-phase to below the phase boundary to an ordered phase region. In addition, SANS experiments provide information about the scattering density and the structure of the precipitates [11–13]. However, there are still some difficulties in extracting the scattering function for all scattering vectors from the rocking curve of a double crystal spectrometer (DCS). The deconvolution procedure involves also the problems of determining the particle-size distribution function [14], the interparticle interference [12] and the correction for slit geometry [15, 16] and multiple scattering [17].

This paper deals with experiments on $\alpha \leftrightarrow (\alpha + \beta)$-phase transitions in the V-H system, which detect the phase boundary by the reduction of the peak intensity and broadening of the rocking-curve of the DCS due to SANS. Experimental neutron transmission data within the temperature interval between 170 °C and 20 °C are fitted to theoretically calculated curves. Similar experiments have been made before at liquid-nitrogen and room temperature [18, 19]. In addition, the Guinier-approximation [20] is used to evaluate the influence of the size of the precipitates on the reflected beam.

2. Experimental Technique and Results

Polycristalline vanadium purchased from MRC with a stated purity of 99.94% was cut to plates of a thickness of 6 mm and degassed for several hours at 1100 °C in the vacuum range of 10^{-10} mbar. Subsequently the plates were doped in a hydrogen gas atmosphere (purity 5 N) at ~ 500 °C. The hydrogen content was determined by measuring the weight of the absorbed gas with an accuracy of ± 5 ppm by weight. The sample parameters are given in Table 1. We have also measured three samples having deuterium contents of 1.14 at%, 2.09 at% and 9.68 at%, respectively. The measurements revealed the same

* Work supported by Fonds zur Förderung der Wissenschaftlichen Forschung (project 3836) and by Bundesministerium für Wissenschaft und Forschung (project Tritium in Metallen).

Reprint requests to Prof. Dr. H. Rauch, Schüttelstraße 115, Atominstitut der Österreichischen Universitäten, A-1020 Wien, Austria.

0340-4811 / 84 / 1100-1077 $ 01.30/0. – Please order a reprint rather than making your own copy.

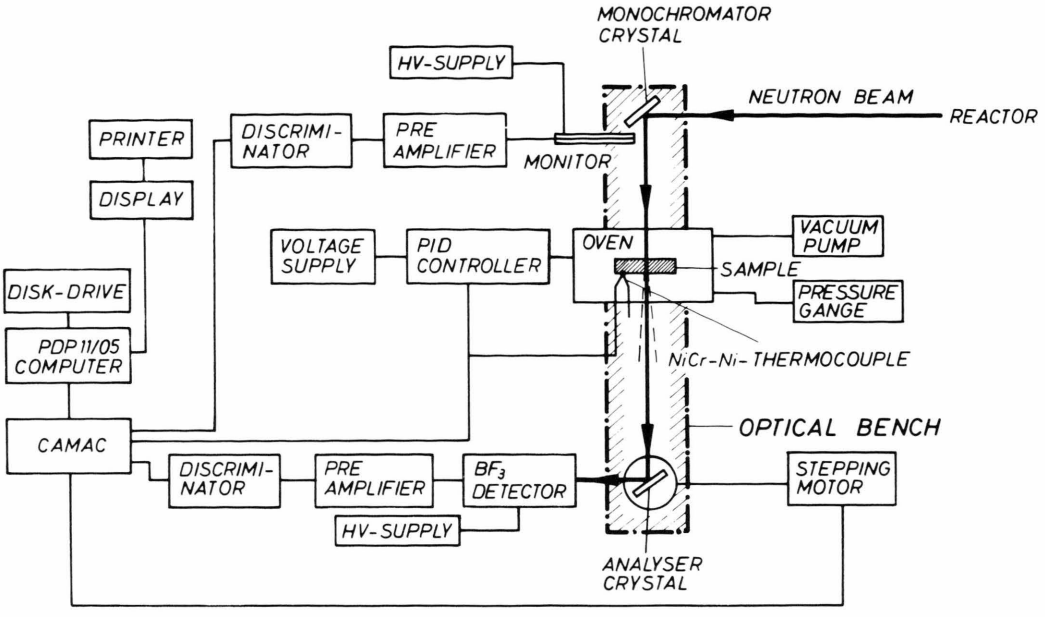

Fig. 1. Sketch of the experimental setup and of the electronic control unit.

characteristics as we found for the hydrogen-loaded samples if the isotope effect is taken into account.

The experimental setup ([19], Fig. 1), which is controlled by a PDP11/05 computer and a CAMAC-system consists of two Bragg-reflecting perfect Si-crystals mounted in a nondispersive arrangement on an optical bench. The monochromator crystal reflects 1.78 Å neutrons at the (4 0 0) plane. The sample was placed within an Al-vacuum chamber and could be heated up to 250 °C. The temperature stability and homogeneity was tested to be better than ± 1 °C. The maximum counting rate was about 2500 cpm. The broadening of the incident beam, which results from scattering by precipitates in the sample was detected by scanning with the analyzer crystal. The stepping motor driving the analyzer crystal allows a minimum step of 1/30 s of arc, corresponding to a scattering vector Q of 0.5×10^{-6} Å^{-1}. The accessible angular range is ± 5′. Data of the rocking curve were collected in the range $Q = 0$ Å^{-1} to 6×10^{-5} Å^{-1} in increments of 4×10^{-6} Å^{-1} and from 6×10^{-5} Å^{-1} to 1×10^{-4} Å^{-1} in increments of 1×10^{-5} Å^{-1}. Each point on a rocking curve was measured for 50 s. The second order contamination of the neutron beam (30%) produces a narrower reflection curve and, therefore, emphasizes the top of the rocking curve. For the data evaluation procedure this contribution has been treated separately.

In order to obtain the characteristic parameters (FWHM, peak intensity and integral intensity) of a rocking curve a least squares procedure was used to fit the theoretical resolution functions to the experimental data. The resolution function results from the convolution of the two Darwin reflection curves of the two crystals [16]. The sample scattering function is assumed to be a Gaussian-shaped curve as predicted by the Guinier-approximation. For the procedure of least squares fitting the half-width, the maximum intensity and the background of the sample scattering curve were varied.

Table 1. Sample parameters.

Sample no.	H-concentration $\frac{H}{V+H} \times 100$	Dimensions (mm)
1	0	47 × 20.5 × 6.2
2	0.58 (2)	47 × 20.5 × 6.2
3	3.39 (2)	61 × 30.5 × 9.2
4	4.32 (2)	47 × 20.5 × 6.2
5	13.02 (2)	47 × 20.5 × 6.2
6	24.89 (2)	47 × 20.5 × 6.2

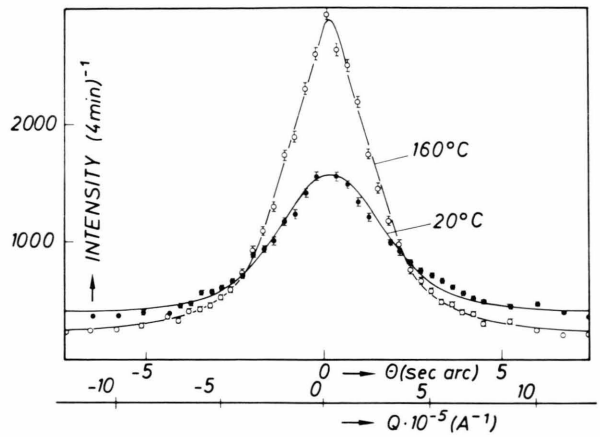

Fig. 2. Characteristic results for the 13.02 at% sample in the pure α-phase (160 °C) and in the ($\alpha + \beta$)-phase (20 °C).

Figure 2 shows a plot of two rocking curves of a 13.02 at% H/H+V-sample in the two phase region at 20 °C and after heating up to 160 °C into the pure α-phase region. The drastic change of the peak height and of the half-width is visible. To limit the influence of statistical errors and external effects these curves are the sum of five consecutive rocking curves.

In Fig. 3 the temperature dependence of the half-width and the peak intensity is shown for three different V-H samples, which were heated from room temperature up to 180 °C. Each point in the plot represents the average value taken from 5 evaluated rocking curves. At 170 °C all the samples are within the α-phase. A synopsis of these values (Fig. 4) can be used for further theoretical considerations, since it may provide information about the scattering cross section of the hydrogen partly trapped within interstitials in the metal.

Figure 4 shows a comparison between the measured and calculated beam attenuation, where the cross section has been taken from a model which describes the α-phase as monatomic free hydrogen atoms having an effective mass M^*.

3. Discussion

The dynamics of hydrogen in the α-phase may be described as a partly free lattice gas because the rest-time at the tetrahedral sites and the jump-time between these sites are comparable [21]. The related hydrogen cross section exceeds the free cross section (σ_{free}) but is smaller than the bound cross section (σ_{bound}) and depends on the dynamic behavior of the hydrogen in the host lattice. The energy and temperature dependence of the cross section according to the gas model has been recalled in a previous publication [19]. The inclusion of oscillatory motions may be described by a Krieger-Nelkin model [22] introducing an effective mass M^*. With this assumption an approximative expression for the cross section is

$$\sigma = \alpha\, \sigma_{\text{free}} ,$$

where

$$\alpha = 4(1 + m_{\text{n}}/M^*)^{-2}$$

with the neutron mass m_{n}. From an optimal fit of the transmitted intensity as a function of the hy-

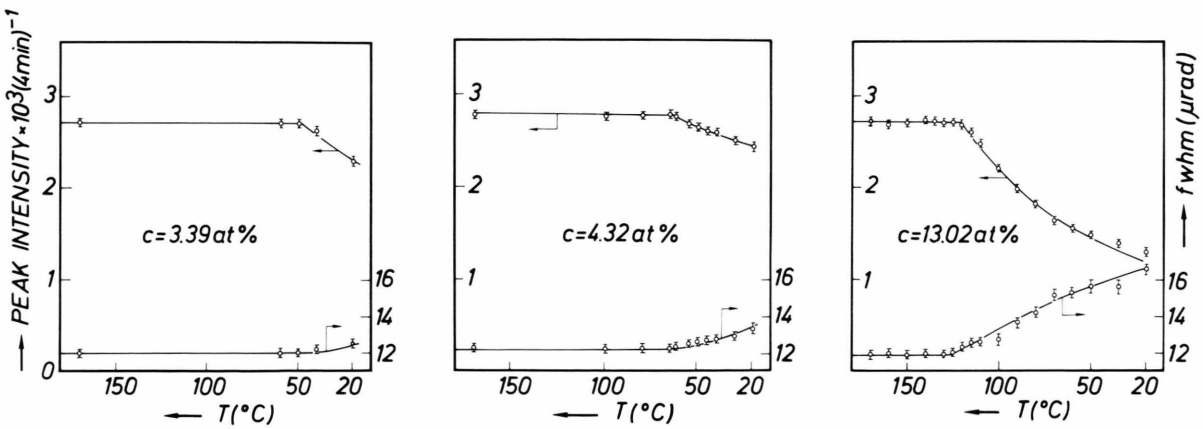

Fig. 3. Peak intensities and half-widths of three different samples as a function of temperature.

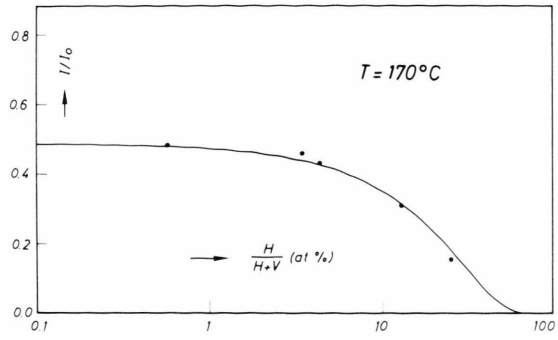

Fig. 4. Peak intensity of the samples in the α-phase as a function of the hydrogen concentration fitted to an effective mass formula.

drogen concentration (Fig. 4) a value of $\alpha = 1.82$ is deduced, giving an effective mass $M^* \cong 2\,m_n$.

A measurement at different neutron wave lengths could yield more information about the binding character of the hydrogen. The dynamics of hydrogen was investigated in detail by means of inelastic neutron scattering [23, 24]. Although the jump-time between the interstitital sites is comparable to the mean rest-time at a site for the vanadium-hydrogen system, the value for the effective mass is surprisingly small; an effect which was also observed for niobium [19], where the binding should be even stronger. The whole scattering function has to be integrated over all possible energy- and momentum-transfers to obtain the total cross section as a function of energy. Unfortunately, no such cross sections have been extracted for the various metal-hydrogen systems.

The measurements in the temperature region between room temperature and 180 °C permit the determination of the $\alpha-\beta$ phase transition due to the beginning small-angle scattering of the β-phase V_2H. This effect reduces the peak intensity and increases the half-width of the rocking-curve of the double-crystal spectrometer (Figure 3). The forward scattering probability of a precipitate with radius R can be written as [17, 12]

$$S(0) = Dp\frac{4\pi}{3}R^3(N_\beta b_\beta - N_\alpha b_\alpha)^2\,,$$

where D is the sample thickness, p the volume fraction of the precipitates and $N_\beta b_\beta$ and $N_\alpha b_\alpha$ the scattering densities of the α- and β-phase, respectively.

The total cross section for small-angle scattering of neutrons with the wavelength λ is given as [11]

$$\sigma_{tot} = \pi R^4(N_\beta b_\beta - N_\alpha b_\alpha)^2\lambda^2/2$$

with the integrated SANS intensity for a sample with thickness D [18]

$$\int I(\theta)_{sas}\,d\theta = I_0(1 - \exp(-ND\,\sigma_{tot}))\,,$$

where I_0 is the intensity of the primary neutron beam and N is the number of precipitates per volume.

Using the Guinier-approximation one finds for the half-width of the small-angle scattering curve $\Delta\theta_{sas}$

$$\Delta\theta_{sas} = \frac{\sqrt{5\ln 2}\;\lambda}{\pi R}$$

which is independent of the number of precipitates. The reflected intensity in dependence of the analyzer angle θ can be written as [25]

$$I_s(\theta) = I_0 A\,f_s(\theta)\,,$$

where A is a constant taking into account intensity-losses due to absorption and incoherent scattering and $f_s(\theta)$ is the superposition of the undeflected part $f_0(\theta)$ given by the double-crystal rocking curve and of the contribution due to SANS smeared by the rocking curve

$$f_s(\theta) = \exp(-N\sigma_{tot}D)\,f_0(\theta) + (1 - \exp(-N\sigma_{tot}D))\,(f_0 * g(\theta))$$

with $g(\theta)$ the small-angle scattering curve averaged over the vertical divergency of the beam.

Considering that the half-width of the small-angle scattering curve $\Delta\theta_{sas}$ is a function of R within the Guinier-approximation it is now possible to compute the half-width of the reflected curve $\Delta\theta_{refl}$ as a function of R for differing cross section values (Figure 5).

For a quantitative treatment, the shape and the size distribution have to be included [14, 12]. The results from other structural analysis (e.g. optical measurements [1]) show that the precipitates have the shape of thin plates which allow a reasonable interpretation of our scattering data. The calculation of the characteristic parameters of the rocking-curves yields a rising particle size with falling temperature and rising concentration of the β-phase V_2H.

A nearly exponential decrease as a function of falling temperature of the peak intensity was also

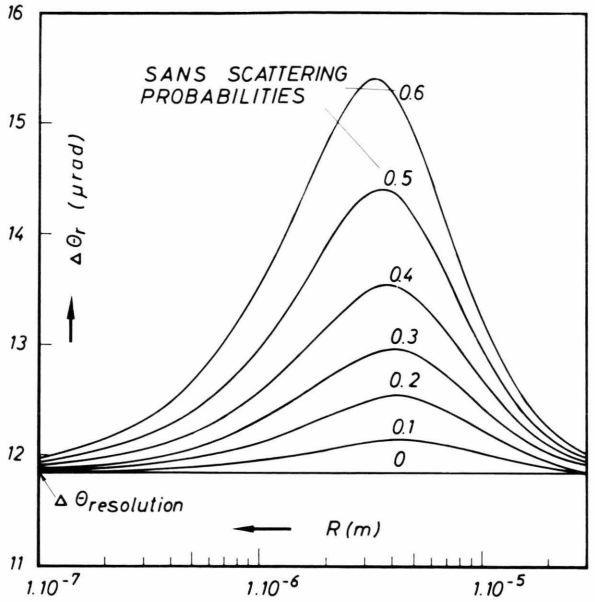

Fig. 5. Plot of the half-width of the rocking curve $\Delta\theta_r$ as a function of the radius of the precipitates for different SANS probabilities.

observed for the β-phase regime. Thus it was possible to determine the phase-transition temperatures of the 3.39 at%, 4.32 at% and 13.02 at% hydrogen samples as $(48 \pm 2)\,^{\circ}C$, $(64 \pm 1.5)\,^{\circ}C$ and $(121 \pm 1)\,^{\circ}C$, respectively. The values are in agreement with the phase diagrams taken from literature [1]. The deviation of the data-points from the calculated decline in the low-temperature region of the 13.02 at% sample is attributed to multiple-scattering effects due to the large volume fraction of the precipitates and therefore increasing total scattering probability [17].

Our results correspond to heating cycles. At the phase-boundary a marked hysteresis effect has been observed by other techniques [26, 27], which we are now investigating in more detail by a real-time SANS experiment.

Acknowledgement

The technical assistance of Mr. H. Bittermann is gratefully acknowledged.

[1] T. Schober and H. Wenzl in: "Hydrogen in Metals II", Topics in Appl. Phys. **29,** 11 (1978), Springer-Verlag, Berlin 1978.
[2] M. A. Pick and R. Bausch, J. Phys. F: Metal Phys. **6,** 1751 (1976).
[3] G. Mair, K. Bickmann, and H. Wenzl, Z. Phys. Chem. **114,** 31 (1979).
[4] V. A. Somenkov, Ber. Bunseng. Phys. Chem. **76,** 733 (1971).
[5] T. Schober, Phys. Stat. Sol. (a) **30,** 107 (1975).
[6] D. G. Westlake and S. T. Ockers, Met. Trans. **6A,** 399 (1975).
[7] H. Wenzl and J. M. Welter, in Current Topics in Material Science, E. Kaldis, Ed., **Vol. 1,** North Holland Publ. Comp., Amsterdam 1978.
[8] O. Buck, D. O. Thompson, and C. A. Wert, J. Phys. Chem. Sol. **32,** 233 (1971).
[9] R. M. Cotts: in "Hydrogen in Metals I", Topics in Appl. Phys., **Vol. 28,** p. 227; J. Völkl and G. Alefeld, Ed., Springer-Verlag, Berlin 1978.
[10] T. Schober and A. Carl: Phys. Stat. Sol. (a) **43,** 443 (1977).
[11] R. J. Weiss, Phys. Rev. **83,** 379 (1951).
[12] G. Kostorz, Neutron Scattering, Academic Press, London 1979, p. 227.
[13] G. Aberfelder, K. Novak, K. Stierstadt, J. Schelten, and W. Schmatz, Phil. Mag. **B41,** 519 (1980).
[14] S. ReFiorentin, J. Appl. Phys. **53,** 245 (1981).
[15] P. W. Schmidt and B. A. Dederov, J. Appl. Cryst. **11,** 411 (1978).
[16] M. Deutsch and M. Luban, J. Appl. Cryst. **11,** 87 (1978).
[17] J. Schelten and W. Schmatz, J. Appl. Cryst. **13,** 385 (1980).
[18] M. Kalanov, S. Sh. Shil'shtein, and V. A. Somenkov, Sov. Phys. Cryst. **18,** 755 (1974).
[19] D. Bader, H. Rauch, and A. Zeilinger, Z. Naturforsch. **37a,** 512 (1982).
[20] A. Guinier: X-ray Diffraction in Crystals, Freeman (1963).
[21] J. M. Rowe, K. Sköld, H. E. Flotow, and J. H. Rush, J. Phys. Chem. Sol. **32,** 41 (1971).
[22] T. J. Krieger and M. S. Nelkin, Phys. Rev. **106,** 290 (1957).
[23] V. Lottner, A. Heim, and T. Springer, Z. Physik **B32,** 157 (1979).
[24] T. Springer, Z. Phys. Chemie **115,** 141 (1979).
[25] J. Kulda and P. Mikula, J. Appl. Cryst. **16,** 498 (1983).
[26] H. Zabel and J. Peisl, Phys. Stat. Sol. (a) **37,** K67 (1976).
[27] H. Zabel and J. Peisl, Acta Met. **28,** 589 (1980).